PERGAMON

International Journal of Heat and Mass Transfer 44 (2001) 633–644

International Journal of HEAT and MASS TRANSFER

www.elsevier.com/locate/ijhmt

# Augmented longitudinal diffusion in grooved tubes for oscillatory flow

Xiaofeng Ye*, Masashi Shimizu

*Department of Mechanical and Environmental Informatics, Tokyo Institute of Technology, 2-12-1, O-okayama, Meguro-ku, Tokyo 152, Japan*

Received 23 August 1999; received in revised form 10 March 2000

**Abstract**

This paper presents the results of an experimental investigation on longitudinal mass diffusion in the tubes roughened by equidistantly-spaced grooves during oscillatory flows of Reynolds number = 210–13,000 and Womersley number = 3.76–10.64. The experiments were conducted in tubes of 6 mm nominal ID using a soluble contaminant of molecular diffusion coefficient = $2.78 \times 10^{-5}$ $cm^2/s$ as the tracer. The experiments show that, in comparison with the smooth one, the grooved tubes could yield an augmentation of up to about two orders of magnitude in effective diffusion rate for our investigation. The present results indicate that, for high Reynolds number flows, the ratio of the volume of core region to that of grooves influence the longitudinal diffusion efficiency in a tuning behavior, the grooved tube in which the core region is equal to grooves in volume performs best in enhancing the axial mass diffusion. 

## 1. Introduction

There are numerous studies concerning the enhancement of axial mass diffusion of contaminant within a long tube when the fluid is subjected to sinusoidal oscillations (e.g. [1–3]). The results of these studies demonstrate that, the effective spread of the contaminant concentration in axial direction is governed by both the axial convection and the radial diffusion and is greater than would be expected from molecular diffusion alone. This mechanism is called "augmented diffusion" and suggests numerous engineering applications where one is interested in accelerating diffusion.

Analytical studies ([4,5]) showed that for a fixed dimension of cross-section and a given Schmidt number, the normalized effective axial diffusivity (the virtual axial diffusion rate attributed to unit tidal displacement and unit oscillation frequency) reaches maximum only for the condition that the radial diffusion time scale and half the oscillation period are comparable. This theoretical prediction was confirmed experimentally by Joshi et al. [2] and Kurzweg [3].

By this line of reasoning, it may be deduced that when the diffusion augmentation of a poorly diffusible contaminant (in general, the molecular diffusivity of liquid soluble material is about four orders of magnitude smaller than that of gases) is desired, the optimum oscillation frequency is so low that the diffusivity possibly approaches zero if all other conditions are held constant. It is therefore of great practical interest to find ways to enhance the diffusion by appropriate modification of the environment.

In this paper, we examined the characteristics of the longitudinal diffusion of a soluble matter during

* Corresponding author.

0017-9310/01/$ - see front matter 
PII: S0017-9310(00)00103-4

**Nomenclature**

| | |
|---|---|
| $a$ | constant based on light absorptivity of tracer |
| $C$ | concentration |
| $D_{\text{eff}}$ | effective diffusivity |
| $D_{\text{mol}}$ | molecular diffusivity |
| $(D_{\text{eff}})_{\max}$ | maximum value of $D_{\text{eff}}$ for given flow parameter |
| $f$ | oscillation frequency |
| $f(\alpha, Re_\delta, Sc)$ | function, cf. Eqs. (7) and (8) |
| $I$ | turbulent intensity |
| $L$ | tube length |
| $M$ | amount of tracer |
| $N$ | number of oscillation cycles |
| $Pe$ | Peclet number, $2R\bar{u}/D_{\text{mol}}$ |
| $r$ | radial coordinate |
| $R$ | tube radius |
| $Re$ | Reynolds number, $2R\bar{u}/\nu$ |
| $Re_\delta$ | Reynolds number based on Stokes layer thickness, $Re/\alpha\sqrt{2}$ |
| $s$ | length of expansion section |
| $Sc$ | Schmidt number, $\nu/D_{\text{mol}}$ |
| $t$ | time |
| $U$ | voltage output of sensor |
| $U_0$ | voltage output of sensor without tracer |
| $u(t)$ | axial velocity |
| $\langle u(t)\rangle$ | ensemble-average velocity, cf. Eq. (5) |
| $u'(t)$ | turbulent velocity |
| $\bar{u}$ | root-mean-square spatially averaged velocity |
| $V_c$ | volume of core region |
| $V_f$ | volume of furrows |
| $\Delta x$ | tidal displacement |
| $z$ | distance |

*Greek symbols*

| | |
|---|---|
| $\alpha$ | Womersley number, $R\sqrt{(\omega/\nu)}$ |
| $\nu$ | kinematic viscosity |
| $\omega$ | angular frequency |

oscillatory flows. Motivation for this investigation is from the fact that there is little published work on the longitudinal dispersion of soluble liquid material during oscillatory flows, whereas the gas transport process mainly concerning the pulmonary ventilation practices has been studied extensively (e.g. [6,7]).

The separated and turbulent flows caused by the unsteady flow in wall-modified tubes have assumed great importance in enhancing mass transfer. In 1973, Bellhouse et al. [8] reported on the success of a membrane oxygenator which utilized pulsatile flows across a furrowed membrane and gave good mass-transfer performance. Sobey [9] made a numerical computation for two-dimensional flow in a channel with sinusoidal wavy walls. Stephanoff et al. [10] qualitatively confirmed the computational results of Sobey by flow visualizations. Nishimura [11] investigated flow and mass-transfer characteristics in such a channel for oscillatory flow with the result showing a maximum mass-transfer enhancement of six-fold in terms of time-averaged Sherwood number, which deduces the high efficiency of the membrane oxygenator developed by Bellhouse et al.

These studies focus primarily on the mass transfer from channel walls to working fluid. However, the longitudinal mass-transport characteristics, which dominate the lateral concentration gradient and therefore influence the overall performance of the system, have not been explored yet.

In the present study, we proposed a modified tube with rectangular grooves equidistantly distributed along the tube axis as a means of promoting the interaction of separated flow with axial convection to enhance longitudinal diffusion during oscillatory flow. First, we examined the diffusion rate within the straight smooth tube over a relatively wide parameter range to investigate the effect of turbulent fluctuations on Taylor dispersion. We then performed the tests with grooved tubes and investigated the characteristics of longitudinal mass diffusion as well as the effect of tube dimension and flow parameter on the diffusion enhancement performance.

## 2. Experiments

### 2.1. Experimental arrangement

#### 2.1.1. Flow system

Fig. 1 shows the experimental arrangement employed in the present investigation. The tube joining the two reservoirs was 2 or 3 m long and made of acrylic pipe which is transparent enough to make use of photoelectric effect in concentration measurements. Inside reservoir A there was a fender plate adjacent to the exit of the cylinder, which plays a role of buffering and straightening flows in combination with the bell mouth at the entrance to the test tube. Reservoir B was open to the atomsphere. The sinusoidal oscillation

of the fluid inside the tube was imposed by a piston driven by a DC servomotor through a Scotch-yoke mechanism. The stroke volume could be varied over the range 0.78–24 $cm^3$. The frequency of oscillation was adjustable from 0 to 3 Hz. Further higher frequency could not be used because of the power limitation of the driving system and the sealing quality of the flow system. The working fluid was city water.

*2.1.2. Geometry of tube*

Both smooth tube and grooved tubes were used in the experiments. The smooth test tube was made of acrylic pipe of 6 mm ID, care was taken in machining and assembling in order to obtain a smooth connection between the tubes and the bell mouth. The grooved test tube was made by assembling the short circular cylinders into an acrylic pipe of 16 mm ID and thus had axially periodically changing circular cross-section. Different configurations of grooved tube were obtained by varying the assemblege of short circular cylinders. Of the grooved tubes, the internal diameters of the contraction section and the expansion section were 6 and 12 mm respectively, the length of contraction section was fixed to be 10 mm with the length of expansion section varying from 1 to 40 mm. Including the smooth one, eight tubes, $S = 0, 1, 3, 5, 7, 10, 20, 40$ mm, were employed in our tests. Prior to the use of a newly assembled test tube, the air within the flow system was removed completely by filling water into the system, which was adjusted to the vertical position then, and imposing some slight vibrations.

*2.1.3. Tracer*

A black dye solution of molecular diffusion coefficient $D_{mol} = 2.78 \times 10^{-5}$ $cm^2/s$ was used as the tracer. Since the molecular diffusivity of this tracer is considerably small in comparison with that of gas (for example, the molecular diffusivity of oxygen in air, $D_{mol} = 0.16$ $cm^2/s$) we have good reason to expect an earlier appearance of the effect of turbulent flows on Taylor dispersion than in gas experiments.

As the dye has a specific gravity greater than the working fluid, the tracer solutions diluted to 10 and 20% concentration were used for smooth test tube and grooved test tubes respectively for the purpose of avoiding density-driven radial mass diffusion to ensure accurate concentration measurement.

*2.1.4. Flow parameters*

The flow parameters selected in this investigation ranged from laminar to turbulent regime. The Reynolds number was from 210 to 13,000 and the Womersley number was from 3.76 to 10.64. Fig. 2 is the mapping of flow conditions with the broken line $Re_\delta = Re/\sqrt{2\alpha} = 550$ proposed by Hino et al. [12] as the critical value for the transition to turbulent oscillatory flow for smooth circular tube.

*2.2. Experimental methods*

*2.2.1. Velocity measurements*

For the diffusion process in a straight smooth tube, the only factor influencing the Taylor diffusion is the presence of turbulent flows provided that the density-driven radial mixing has been eliminated by appropri-

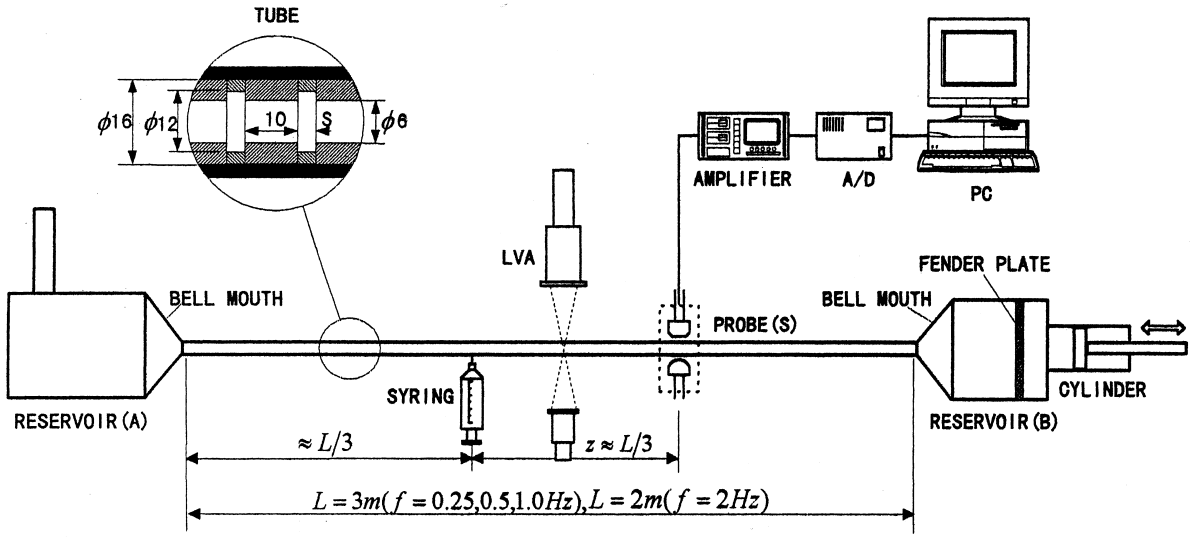


Fig. 1. Schematic diagram of experimental arrangement.

ate means. In order to investigate the effect of turbulence on Taylor diffusion, measurements were performed for the velocity component in axial direction using a LDA (laser-Doppler anemometer) working in the forward-scatter mode. Measurements were taken near the midpoint of the test tube with distance between the measurement point and the tube end reasonably great ($>170$ ID) so that there should be no influence of the end effect in the velocity data. The output of the signal processor of LDA system was digitized by a 12-bit A/D converter at a sampling interval of 0.001 s, the turbulence intensity were calculated afterwards.

*2.2.2. Concentration measurements*

The variation of tracer concentration was determined by measuring the intensity decrement of the light beam (from a light emitting diode) directed along the tube diameter perpendicular to the tube axis. The light detector at the opposite side of the tube was a photodiode with the peak-sensitive wavelength of 560 nm (Model BS500B, SHARP Co., LTD., Japan). Calibration was made of the concentration-sensor output, the data fit reasonably to Beer's law (see Fig. 3).

The concentration measurements were carried out at the point about one-third of the total tube length from the tracer injection point which is also equal to about one-third of the tube length from reservoir B (see Fig. 1). We took this measurement configuration in order to ensure the largest number of concentration data unaffected by the end effect of diffusion (which will be explained later), recognizing the fact that the end effect of diffusion spreads in axial direction at the same speed as original diffusion.

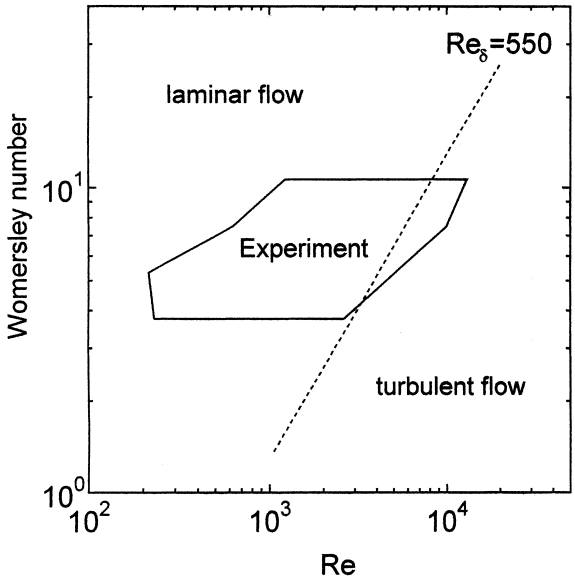


Fig. 2. Mapping of flow conditions.

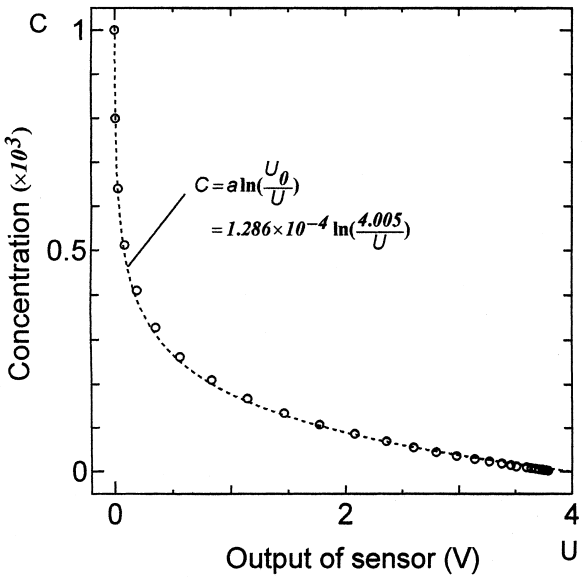


Fig. 3. Concentration–voltage calibration curve of photoelectric sensor.

In order to obtain a pulse-like initial concentration distribution of tracer, injections were executed by an automatic injection system at the oscillatory phase of 270°. As it was the very moment when the fluid was at rest (more exactly, the mean fluid flux over the cross-section is zero) with the maximum displacement, the effect of the disturbance caused by injection on the flow inside the test tube is considered to be negligible.

To improve the measurement accuracy, we used three sensors (their interspacing was 2–5 cm) and took the average value as the result of each measurement.

*2.2.3. Determination of effective diffusivity*

As suggested first by Taylor [13], the diffusion of soluble matter in a moving solvent can be described by means of a virtual coefficient of diffusion which represents the combined action of velocity profile over the cross-section of the tube and molecular diffusion in radial direction. In the case of oscillatory flow, the enhanced diffusion process can be treated as a one-dimensional axial diffusion problem by replacing the molecular diffusivity term in the basic diffusion equation with the so-called effective diffusivity whose value depends on the macroscopic properties of flow such as mean axial flow velocity, tube diameter, Schmidt number, also tidal displacement and Womersley number.

The basic equation for one-dimensional dispersion is

$$\frac{\partial C}{\partial t} = D_{\text{eff}} \frac{\partial^2 C}{\partial z^2} \tag{1}$$

where $D_{\text{eff}}$ is the effective diffusivity and have been used to represent the virtual longitudinal diffusion rate in oscillatory flows.

When a bolus of tracer were injected into the test tube in a flash, the initial concentration distribution would be approximately pulse-shaped and we will have the time variation of concentration

$$C(z, t) = \frac{M}{2\sqrt{\pi D_{\text{eff}} t}} \mathrm{e}^{-\frac{z^2}{4D_{\text{eff}} t}} \tag{2}$$

where $z$ is the distance between the injection point and the measurement point.

Noticeable scatter arose when using all the concentration data at the same phase as that of injection to fit Eq. (2) to determine $D_{\text{eff}}$, especially for large tidal amplitude. Tanaka et al. reported the similar trouble in his investigation [14].

This uncertainty is produced by the inconsistency of the real tube to the model from which Eq. (2) was developed. In contrast to the terse form of Eq. (2) which was based on the infinitely long tube, only superfluous expression in the form of a series can be obtained for the case of tube of finite length because the Fourier integration over a finite area can only yield a series-form result. Though, theoretically, the series-form expression for the concentration variation can be utilized in the least-squares fitting operations to determine $D_{\text{eff}}$, it is nearly impossible in practice to perform such operation because of the inadequate computing ability of common PC machines.

The discrepancy between the concentration data and the theoretical prediction (Eq. (2)) can be considered to be the result of a special end-effect which is produced due to the difference in diffusion rate between the test tube section and reservoirs. Since the working fluid of present experiments can be treated as an impressible fluid, as the fluid is convected back and forth during oscillation, this kind of end-effect spreads axially at the same speed as that of original diffusion provided that the tube has a macroscopically uniform cross-section along the axis.

The end-effect of diffusion and that of velocity are quite different in that the former spreads axially in Taylor or Taylor-like mechanism while the latter does not. So the end-effect of diffusion can not be eliminated by, for example, positioning the measurement spot far enough from the ends of test tube.

Another feature of the end-effect of diffusion is that before the injected tracer reaches the ends of the test tube there is no such end-effect within the tube. For both, the injection point and the measurement spot are at some distance from the ends of tube, there are certainly some uncontaminated concentration data. To extract these *pure* data, transformation has to be executed on Eq. (2). Taking the logarithm of Eq. (2), we

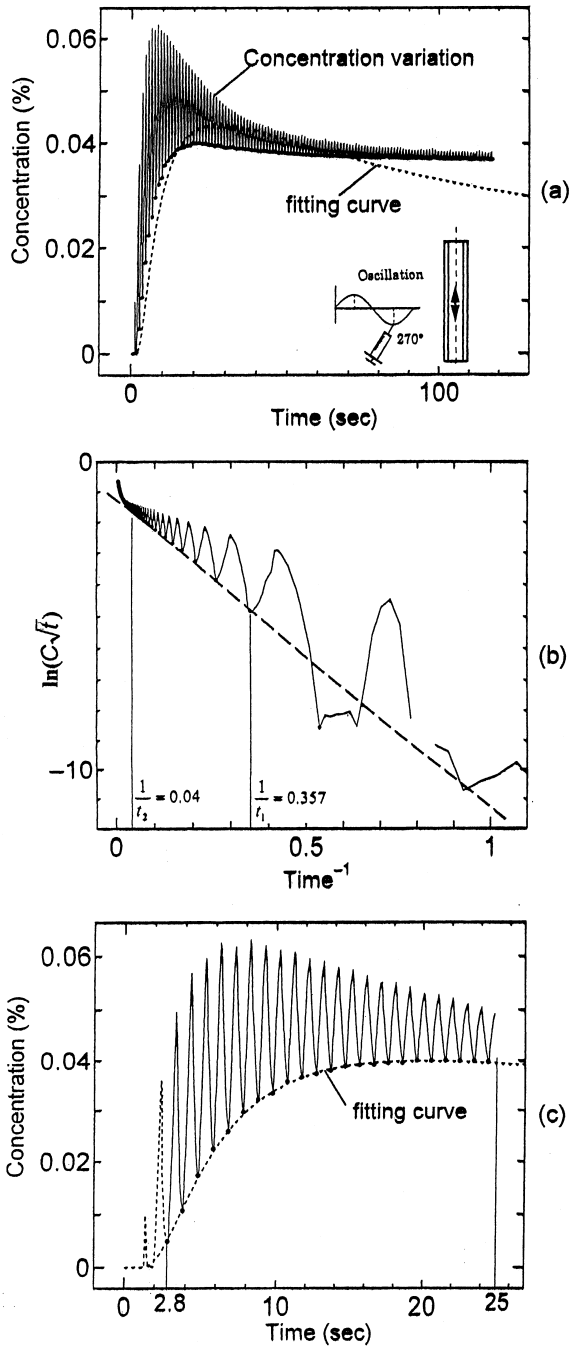


Fig. 4. An example of extracting the uncontaminated data: (a) fitting of the data at the injection phase to Eq. (2); (b) determination of the range in which the concentration data are not influenced by end-effect; (c) fitting of the uncontaminated data to Eq. (2).

have

$$\ln(C\sqrt{t}) = \ln\left(\sqrt{t}a\ln\left(\frac{U_0}{U}\right)\right) = \ln\left(\frac{M}{2\sqrt{D_{\text{eff}}}}\right) - \frac{z^2}{4D_{\text{eff}}}\frac{1}{t} \tag{3}$$

Eq. (3) indicates that, if there were no end-effect of diffusion, the concentration data at the injection phase would fall on a straight line with slope equal to $-z^2/4D_{\text{eff}}$ when plotted in $\ln(C\sqrt{t}) \sim 1/t$ plane. Fig. 4 shows an example of the effective diffusivity determination using the so-called pure data.

In Fig. 4(a), the fitting curve is obtained using the least-squares fitting method based on all the concentration data at the injection phase. It is seen that the data points do not fall on this curve. In Fig. 4(b) plotted are the same data as that in Fig. 4(a) but in $\ln(C\sqrt{t}) \sim 1/t$ coordination system. The upsweeping of the points for $1/t \leq 1/t_2$ is considered to be due to the end-effect of diffusion.

In contrast to the discrepancy of the points for $1/t \leq 1/t_2$, the deviation of the marked points from the straight line for $1/t \geq 1/t_1$ arises because, in the first several cycles, the tracer concentrations at the injection phase are so low that the values of $\ln(U_0/U)$ are near zero and the values of $\ln C = \ln(\ln(U_0/U))$ are thus very sensitive to measurement errors which are liable to arise because the concentration–voltage calibration curve is nearly vertical as the concentration approaches zero (see Fig. 3).

The points show fairly good linearity for $1/t_2 \leq 1/t \leq 1/t_1$ in Fig. 4(c). This indicates that the concentration data at $t_1 \leq t \leq t_2$ fit well to Eq. (2) and should be used to determine the effective diffusivity.

## 3. Results and discussion

### 3.1. Straight tube

We performed first the experiments with straight smooth tube in order to get the fundamental information of augmented longitudinal diffusivity which is necessary in evaluating the effectiveness of grooved tubes. The smooth tube employed was 3 m in length for the 0.25, 0.5, 1.0 Hz runs and 2 m for the 2.0 Hz runs.

#### 3.1.1. Turbulence in oscillatory flow

The measurements of velocity were executed at the radius location $r \approx 0.5R$. The velocity fluctuation is defined as

$$u_i'(t) = u_i(t) - \langle u(t)\rangle \tag{4}$$

where $\langle u(t)\rangle$ is the ensemble-average velocity and is obtained by the segmented velocity data for each cycle $u_i(t)$ $(i = 1, 2, \ldots, N)$, i.e.

$$\langle u(t)\rangle = \frac{1}{N}\sum_{i=1}^{N} u_i(t) \tag{5}$$

The turbulence intensity is calculated as

$$I = \sqrt{\langle u_i'(t)^2\rangle} \tag{6}$$

The calculated values of turbulence intensity are shown in Fig. 5. It may be seen that, the tendency of the turbulence intensity for four oscillation frequencies can be represented by a single curve, indicating that the turbulence intensity is dependent on $Re_\delta$. Although the increase of turbulence intensity becomes fast suddenly when $Re_\delta$ exceeds about 550, turbulent fluctuation exists undoubtedly over the whole flow parameter range in the present investigation. The increment in turbulence intensity is steep for $550 < Re_\delta < 850$, whereas this increment falls when $Re_\delta$ exceeds about 850 probably due to limitation of the tube cross-section which restrains the bursting and diffusion of large turbulent eddies.

#### 3.1.2. Effect of turbulence on longitudinal diffusion

Fig. 6 shows the effective diffusivities plotted against Reynolds number with the solid lines representing the theoretical predictions for laminar flow values based on the analytical investigation of Watson [5]. It is seen that, except a few data for frequency of 0.25 Hz, the points for $D_{\text{eff}}$ deviate from the corresponding theoreti-

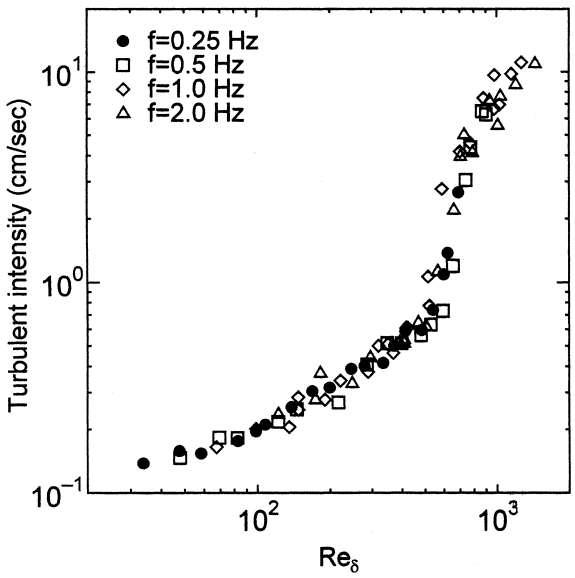


Fig. 5. Variation of turbulence intensity at the radius $r \approx 0.5R$ with $Re_\delta$.

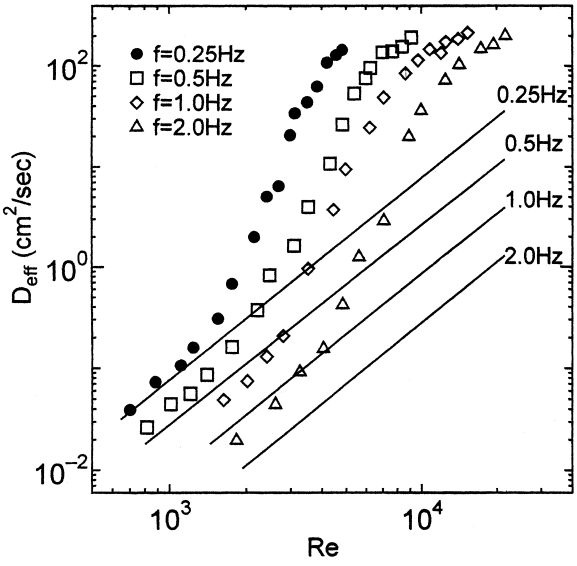


Fig. 6. Results of effective diffusivity for smooth tube.

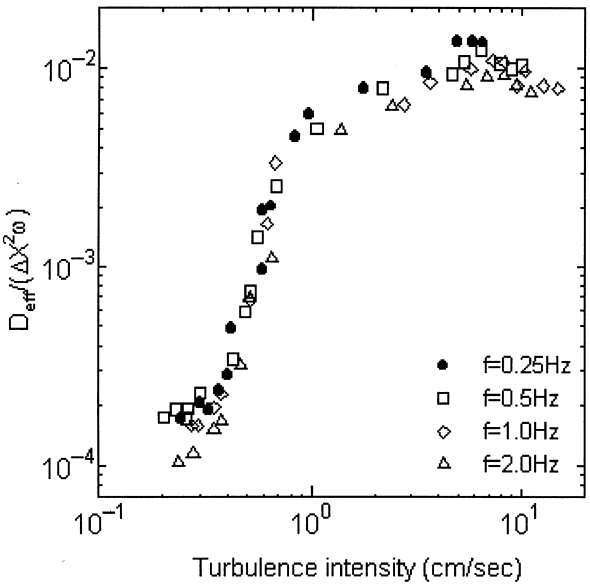


Fig. 7. Correlation of the normalized diffusivity to turbulent intensity.

cal predictions and the deviations become noticeable as the Reynolds number increases. This indicates that the diffusion process is influenced and dominated by the turbulent diffusion as the Reynolds number increases.

In previous studies on the mass diffusion in oscillatory laminar flows, it has been shown that the virtual longitudinal diffusion is the result of the interaction of axial convection and radial diffusion and can be described by [5]

$$D_{\text{eff}} = D_{\text{mol}}\left(1 + f(\alpha, Sc)Pe^2\right) \tag{7}$$

where the first term in the right hand side is responsible for the contribution of molecular diffusion of the tracer and usually negligible for diffusion process in liquid fluid, the second term accounts for the interaction of axial convection with radial diffusion. Eq. (7) shows that, through an appropriate normalization treatment, all the data for axial diffusion for a single tracer can be predicted by a single curve.

In the case of turbulent flows, the second term in the right hand side of Eq. (7) will be no longer a function only of the Womersley number $\alpha$ but a function of $\alpha$ and other flow parameters such as Reynolds number because the lateral mixing is influenced by turbulent diffusion. For the present experiments for smooth tube, we found that the results can be correlated by

$$D_{\text{eff}} = D_{\text{mol}}\left(1 + f(\alpha, Re_\delta, Sc)Pe^2\right) \tag{8}$$

with

$$f(\alpha, Re_\delta, Sc) = \frac{8.14\times10^{-3}}{\alpha^{2.4}}\exp\left[\frac{-1.94\times10^{12}\left(1+4.97\times10^{-4}Re_\delta\right)}{Re_\delta^2\left(Re_\delta-1.69\times10^3\right)^2+7.18\times10^5\left(Re_\delta-5.83\times10^2\right)^2+4.3\times10^{10}}\right]$$

The molecular diffusion coefficient of the tracer we used is so small that $f(\alpha, Re_\delta, Sc)$ can be considered as the contribution of the turbulent mixing to the longitudinal diffusion.

In comparison to liquid tracer, the transport process of gas during oscillatory flow of air seems somewhat strong to the influence of turbulence owing to its relatively large molecular diffusion coefficient. Joshi [2] reported in his gas transport experimental research that no obvious effect of turbulent flows on Taylor diffusion was observed for flows of $Re_\delta$ up to 300. In another gas transport investigation employing a similar system [15], however, the existence of turbulent flows at $Re_\delta = 300$ was confirmed.

Fig. 7 shows the correlation of longitudinal diffusivity to turbulent intensity. The data for diffusivity here were normalized using the factor $\Delta x^2\omega$ for its rationality, because during oscillation both the concentration gradient in radial direction and the area of the contacting surface of the concentration boundary layer and core are proportional to the tidal displacement, and $\omega$ is a measure of the number of oscillation cycles per unit time. The data of Fig. 7 indicate that for weak turbulent flows the longitudinal diffusion rate becomes great as the turbulent intensity increases, while when the turbulent intensity exceeds a certain value the lateral mixing raised by the turbulent diffusion worsen the effi-

ciency of axial diffusion, exhibiting the tuning effect of turbulent flows. Similar to the diffusion in laminar oscillatory flow, the peak of the normalized effective diffusivity corresponds to the circumstance that the radial mixing time scale is comparable to half the oscillation period.

It is also seen from Fig. 7 that, though the scatters make the location of peaks vague to some extent, the normalized effective diffusivities yield their maximum values in a manner that higher is the oscillation frequency the higher will be the peak-corresponding $Re_\delta$. This is because the turbulence intensity is a monotonic increment function of the Stokes layer Reynolds number and the optimum condition for higher frequency thus corresponds to higher $Re_\delta$.

Nishida [15] investigated experimentally the longitudinal transport of gas in a straight smooth tube using the flow parameter over laminar and turbulent flow regimes. The results showed a considerable transport augmentation due to the turbulent diffusion. It is difficult, however, to make a direct comparison between Nishida's investigation and our present work because of the essential difference between the two works. The factor contributing to this difference is not only the difference in the molecular diffusivity between the tracers used, which influence the strength and the acting range of the molecular diffusivity, but also the unique feature of the oscillating gas flow is that, during oscillation, the phase and the tidal displacement are position dependent due to the compressibility of the tracer; the effective diffusivity determined experimentally is a resultant reflection of the dispersions contributed by the oscillating flows of different tidal displacements and different phases lags over the whole tube length. In spite of this, it is found that the data of Nishida's experiments yield a maximum effective diffusivitiy of approximately the same order in value as that of ours (taking into account the ratio of amplitudes of cross-sectional mean velocity to amplitudes of piston velocity) if normalized by $\Delta x^2\omega$.

### 3.2. Grooved tubes

#### 3.2.1. Features of diffusion in grooved tubes

For simplicity we approximate the grooved tube in a two-layer model with the tube divided into a core region having the same cross-section dimension as contraction sections, and an outer layer region composed of the ring-shaped furrows. Under the condition of oscillation, the fluid in core region is, in view of macrostructure, convected back and forth like in smooth tube, with the fluid in outer layer region recirculating within furrows (eddy-like internal motion). The disturbing effect of the roughened tube wall makes the radial velocity profile of the core region blunt, yielding a large radial velocity gradient between the two regions (refer to Fig. 8).

The lateral mass exchange and mixing take place between the two regions due to flow separation, turbulent entrainment, vortex ejection and, of course, molecular diffusion. The turbulent flows in the core region play an important role of leveling concentration distribution over the cross-section and make the mixing more efficient. Concerning the fluid in furrows, the concentration distribution is leveled greatly by the recirculating motions in combination with turbulent fluctuations. The mass mixing between such two regions is something like the heat transfer between two layers of material of excellent heat conductivity with the exception that, for the mass mixing during oscillatory flow, the ejecting of vortex from furrows into the mainstream, which is considered to contribute greatly toward the lateral diffusion, occurs as the flow reverses. These approximations are consistent with the observations in the present investigation and other related experimental works (e.g. [11,16]).

Now we have a circumstance that as the fluid in core region is convected in axial direction back and forth, lateral mixings occur with high efficiency in the vicinity of the interface of the core region and the outer layer region, where both the velocity gradient and concentration gradient are large.

As the forgoing approximation implies, despite the peculiar geometry of grooved tube, the diffusions are

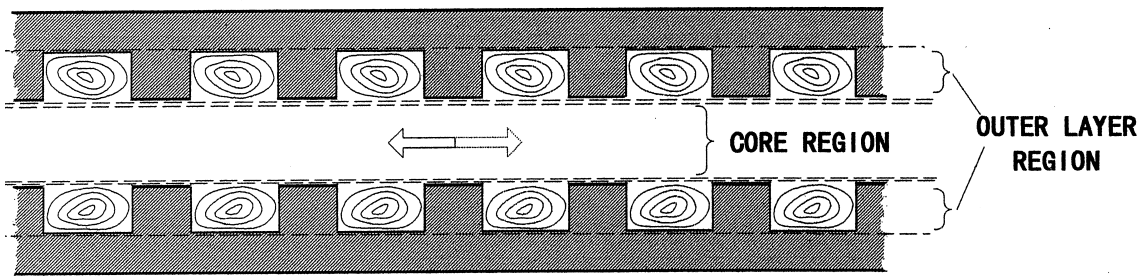


Fig. 8. Simple model for grooved tube.

similar, in mechanism, to that in smooth tube. Thus the factor used to normalize the effective longitudinal diffusivity for smooth channel is still valid reasonably for grooved tubes.

It should be noted that the validity of the so-called two-layer model is questionable for very low Reynolds number flows and for the tubes having relatively long expansion sections, because under such conditions no complete recirculating motion and strong turbulence could be expected.

*3.2.2. Effects of flow parameters*

Experiments were conducted with grooved tubes over the same range of flow parameter and in the same operation sequences as with smooth tube. Fig. 9 shows the results in dimensionless form plotted against the Stokes layer Reynolds number $Re_\delta$ which was calculated using the internal diameter of the contraction section. Though there are other appropriate forms of Reynolds number, for example, the Reynolds number based on the average cross-section of the channel as proposed by Nishimura et al. [11], we used the Reynolds number mentioned above because a grooved tube is modified from a smooth tube by fitting furrows equidistantly along the axis and evaluate the effectiveness of a grooved tube by comparing its effective diffusivity with the corresponding smooth tube value.

Fig. 9 shows that both flow and geometric par-

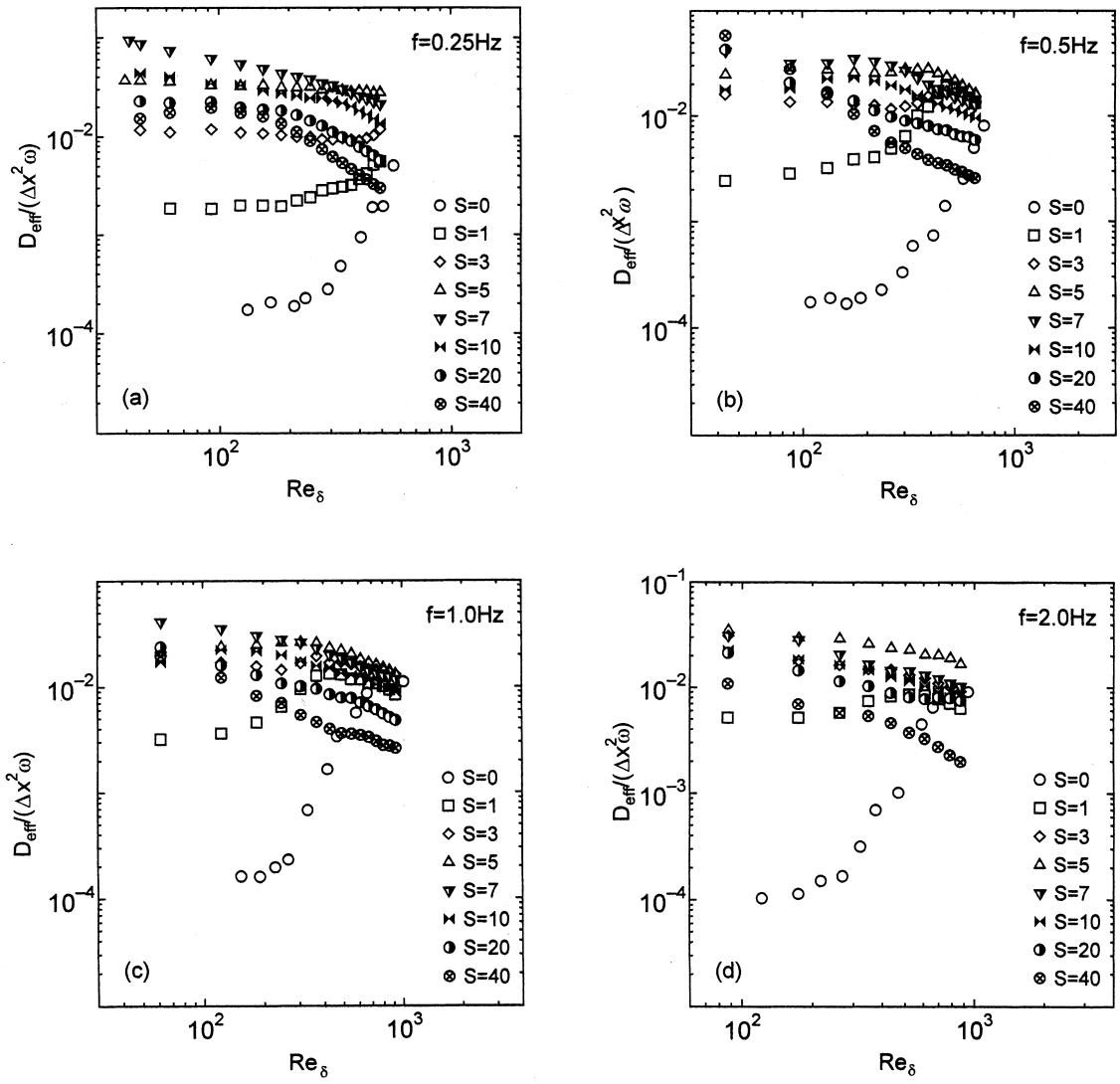


Fig. 9. Results of effective diffusivity for grooved tubes.

ameters influence the effectiveness of grooved tubes considerably with the greatest augmentation of about two orders of magnitude for the present experimental system. Since every figure corresponds to a fixed frequency, the shape of curves indicates the dependence of effective diffusivity on the tidal displacement of oscillation. Except a few data for the tube of $S = 20$ and 40 mm at the frequency of 0.25 Hz, the points in four figures vary in a similar manner, implying that the effect of frequency is, in comparison to the effects of the tidal volume and the geometry of tube, small. This makes the performance of the grooved tubes insensitive to oscillation frequency and facilitates the parameter setting in practical applications.

Though distorted by the experimental error to some extent, from the tendency of the experimental data we have reason to believe that every set of data for a given tube has its peak though some peaks are obviously located out of the range of the present test parameters.

The information about the dependence of peak-corresponding $Re_\delta$ on tube geometry can be utilized in designing application devices. The results of our experiments indicate that the grooved tube with relatively long expansion section may be used in, for example, blood oxygenators and bioreactors where the viscous liquids containing shear-sensitive biomaterials such as animal cells and plant cells are processed.

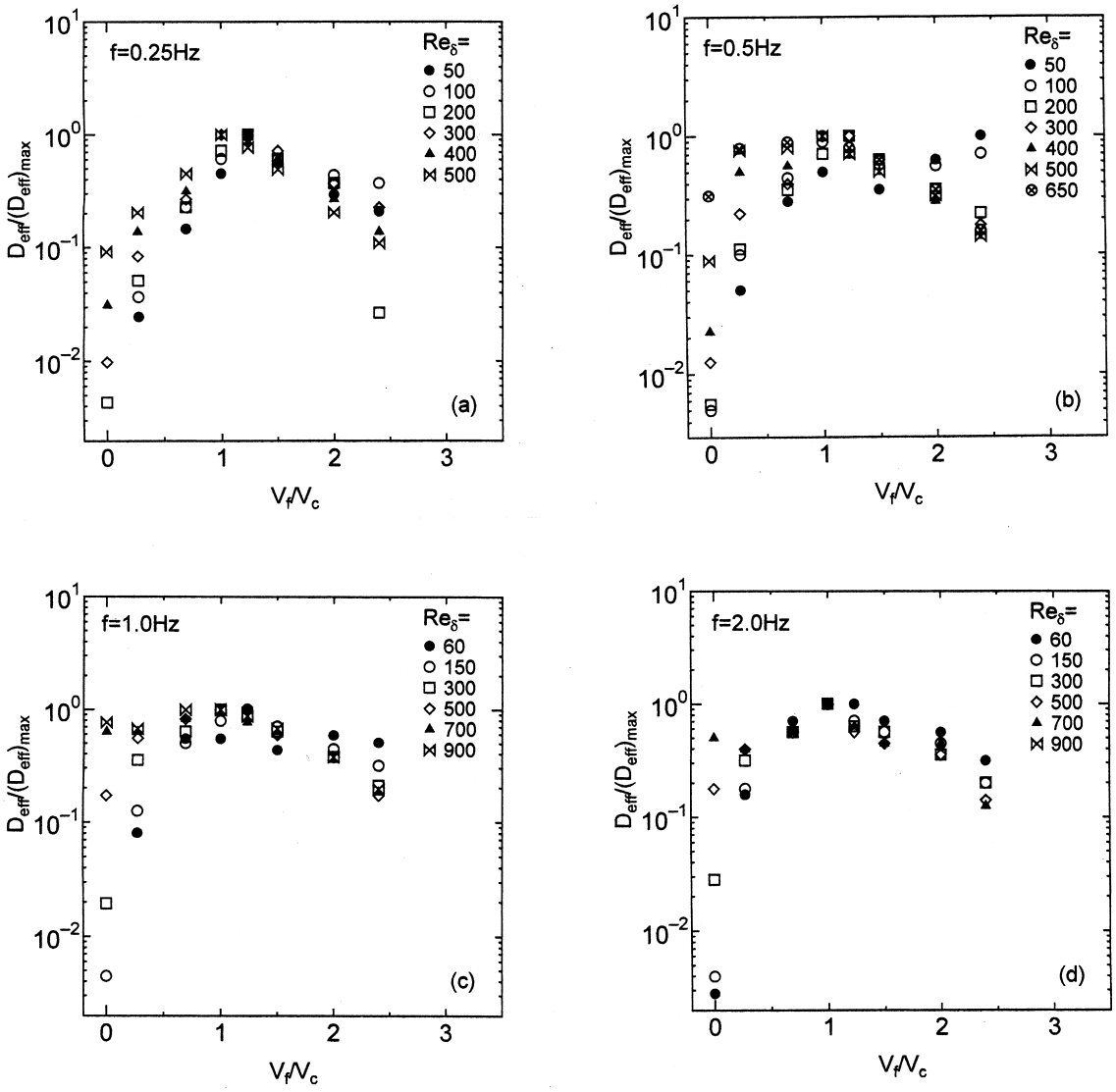


Fig. 10. Effect of tube geometry on effective longitudinal diffusivities.

By comparison with other three figures, the left hanging down of the curves for the grooved tubes of $S = 20$ and 40 mm in Fig. 9(a) is exceptional. Tests were made of the distance over which the tracer-containing fluid was convected by one oscillation cycle and the result showed that, under the condition of small tidal displacement and frequency of 0.25 Hz, the tracer in a contraction section could not be transmitted satisfactorily to the adjacent. In other tests with higher oscillation frequencies, this phenomenon was not observed.

*3.2.3. Effects of tube geometry*

It is of interest to note that even the tube roughened slightly by the narrow furrows ($S = 1$ mm) can enhance the longitudinal diffusion greatly (see Fig. 9). Though it is sure that the geometry of the grooved tube influences the longitudinal diffusivity, the pattern of the influence is hard to grasp due to the overlapping of the effect of flow parameters and tube geometry. From the essential mechanism of augmented diffusion in oscillatory flows, it is reasonable to anticipate that the lateral mixing and therefore the longitudinal diffusion rate are dominated intrinsically by the ratio of the volume of core region to furrows. As the Reynolds number increases, the efficiency of the exchange between the two regions will reaches gradually its limit and the intrinsic effect of the tube geometry will become visible. In Fig. 9, when the Reynolds number is large enough, the ranking of the grooved tubes in regard to the normalized effective diffusivity becomes gradually fixed.

Using the dimensionless effective diffusivity to evaluate the performance of the tubes, we see that for relatively low Reynolds number flow, the most efficient tube is that with relatively long expansion section; as the Reynolds number increases, the length of the expansion section corresponding to the most efficient grooved tube decreases with the asymptotic value $S = 5$ mm.

The effect of the tube geometry is demonstrated explicitly in Fig. 10 where the vertical coordinate was normalized so that the maximum value for each set of data is approximately 1.0. The phenomenon that for large Reynolds number the grooved tube of $S = 5$ mm performs most efficiently is of interest because it corresponds to the condition that the ratio of the volume of furrows to fluid core, $V_f/V_c$, equals 1.0. The mass exchange and/or mixing between two regions contacting with each other is analogous to the charge/discharge between two electric condensers provided that the concentration distributions in the two regions are uniform respectively. It can be simply verified that when the two condensers are equal in capacity, the amount of the electric charge exchanged between the two condensers of different initial voltage is largest.

Figs. 9 and 10 show that when the Reynolds number is not large enough, the most efficient transport process is realized by the tube of $S > 5$ mm. In the low Reynolds number flows, owing to the relatively weak turbulence and flow separation, the completeness of the radial mixing is lower than would be expected in its limit case, in other words, the equivalent volume participated in the radial mixing is smaller than the calculated and, therefore, a larger volume of furrows than that for $S = 5$ mm would be needed to carry out the most efficient lateral mixing.

## 4. Concluding remarks

We conducted the experiments on the augmented longitudinal diffusion of soluble matter during oscillatory flows in straight smooth tube and grooved tubes.

The result of the experiments with smooth tube indicated that the Taylor dispersion was influenced by turbulent flows greatly. In the present investigation, all the experimental data, except a few data for very low frequency and small tidal displacement, deviate from the theoretical predictions by the laminar diffusion model. Due to the very small molecular diffusivity of the tracer used in our tests, the effects of turbulent diffusion on longitudinal dispersion appear much earlier than that in gas experiments of other investigators.

The experiments with grooved tubes show that the ring-shaped furrows distributed equidistantly along the tube axis play a very important role in enhancing longitudinal mass diffusion. By using the grooved tubes, high efficient diffusion can be expected even at considerably low Reynolds number which would yield only a poor longitudinal diffusion in the case of smooth tube.

For the diffusion in grooved tubes, both flow parameter and tube geometry influence the lateral mixing and, as the Reynolds number increases, the effect of oscillation frequency becomes weak whereas the ratio of the volume of furrows to core region influence dominantly the efficiency of the tubes in enhancing longitudinal diffusion. For high Reynolds number flows, the most efficient axial diffusion is realized by the tube of $S = 5$ mm, of which the volumetric ratio is equal to 1.0.

The dependence of the behavior of longitudinal diffusion in grooved tubes on molecular diffusivity has not been tested in our experiments since we used a single tracer. The experiments with other tracers are under projection.

## References


[1] P.C. Chatwin, On the longitudinal dispersion of passive contaminant in oscillatory flows in tubes, J. Fluid Mech. 71 (1975) 512–527.

[2] C.H. Joshi, R.D. Kamm, J.M. Dragen, A.S. Slutsky, An experiment study of gas exchange in laminar oscillatory flow, J. Fluid Mech. 133 (1983) 245–254.

[3] U.H. Kurzweg, M.J. Jaeger, Tuning effect in enhanced gas dispersion under oscillation conditions, Phys. Fluids 29 (1986) 1324–1326.

[4] U.H. Kurzweg, Enhanced heat conduction in oscillating viscous flows within parallel-plate channel, J. Fluid Mech. 156 (1985) 291–300.

[5] E.J. Watson, Diffusion in oscillatory pipe flow, J. Fluid Mech. 133 (1983) 233–244.

[6] M. Nishida, Y. Inaba, K. Tanishita, Gas dispersion in a model pulmonary bifurcation during oscillatory flow, Trans ASME, J. Biomech. Engng. 119 (1997) 309–316.

[7] R.D. Kamm, Gas transport during oscillatory flow in a network of branching tubes, Trans ASME, J. Biomech. Engng. 106 (1984) 315–320.

[8] B.J. Bellhouse, F.H. Bellhouse, C.H. Curl, T.I. MacMillan, A.J. Gunning, E.H. Spratt, S.B. MacMurray, J.M. Nelems, A high efficiency membrane oxygenator and pulsatile pumping system and its application to animal trials, Trans. Am. Soc. Artif. Internal Organs 19 (1973) 72–78.

[9] I.J. Sobey, On flow through furrowed channels. Part 1. Calculated flow patterns, J. Fluid Mech. 96 (1980) 1–26.

[10] K.D. Stephanoff, I.J. Sobey, B.J. Bellhouse, On flow through furrowed channels. Part 2. Observed flow patterns, J. Fluid Mech. 96 (1980) 27–32.

[11] T. Nishimura, A. Tarumoto, Y. Kawamura, Flow and mass transfer characteristics in wavy channels for oscillatory flow, J. Heat and Mass Transfer 30 (1987) 1007–1015.

[12] M. Hino, M. Sawamoto, S. Takasu, Experiments on transition to turbulence in an oscillatory pipe flow, J. Fluid Mech. 75 (1976) 193–207.

[13] G.I. Taylor, Dispersion of soluble matter in solvent flowing slowly through a tube, Proc. R. Soc. London Ser. A 219 (1953) 186–203.

[14] G. Tanaka, Y. Ueda, K. Tanishita, Augmentation of axial dispersion by intermittent oscillatory flow, Trans ASME, J. Biomech. Engng. 120 (1998) 405–415.

[15] M. Nishida, H. Fujioka, T. Kowatari, K. Tanishita, Effect of turbulence on the Taylor dispersion in oscillatory flow, Advances in Bioengineering, ASME BED 22 (1992) 211–214.

[16] M.E. Ralph, Oscillatory flows in wavy-walled tubes, J. Fluid Mech. 168 (1986) 515–540.